# Heat TransportAnd Electronic Scattering QuantumVia 2D System

**Bendoura Abdallah 1**
abdallahka79@gmail.com
**Laboratory of Energy, Environment, and Information Systems Ahmed Draya University, Adrar (Algeria).**
**Tigrine Rachid 2**
tigriner@univ-adrar.edu.dz
**Laboratory of Energy, Environment, and Information Systems, Ahmed Draya University, Adrar, Laboratory of Physics and Quantum Chemistry, University MouloudMammeri of Tizi-Ouzou, P.O. Box No. 17 RP, 15000 Algeria**
**Zouaneb. Aicha 3**
zouaneb.aicha@univ-adrar.edu.dz
**Laboratory of Energy, Environment, and Information Systems, Ahmed Draya University, Adrar (Algeria).**
**Bouchareb Sansabilla 4**
san.boucha@univ-adrar.edu.dz
**Laboratory of Energy, Environment, and Information Systems, Ahmed Draya University, Adrar (Algeria).**

**Received: 01/2024, Published: 01/2024**

**Abstract:**

We study thermal conductivity and electronic ballistic coherent transport via perturbed 2D nanostructure because these areas have potential applications in quantum physics and microelectronic devices, among other fields. The term "inhomogeneous 2D nanostructure" refers to the electronic scattering caused by an integrated defect in domain boundaries. Localized electronic states and the scattering of an incident electronic wave result from the translation symmetry breaking caused by scattering in a perturbed system structure. The distinctive electronic characteristics of atomic sites that make up a comprehensive representation of defect domain boundaries are computed using the matching technique related to the Tight Binding technique. Relationship spectrum variations corresponding to hopping integral changes in the domain boundary were computed. It was demonstrated that the spectra's physical characteristics are sensitive to change of thephysical parameters at the neighbord of the defect.

**Keywords:** Electronic properties; Matching method, quantic 2D system Green functions, Scattering phenomena,EDOS, Tight Binding method, Landaueur-Büttiker formalism
**PAC Codes:** 85.35.-p, 73.63.Nm, 31.15.xf
**DOI Number: 10.48047/nq.2024.22.1.NQ24017** **NeuroQuantology 2024; 22(1):172-183**



## I.Introduction

Reliable techniques for forming nanostructures are essential to the advancement of the nanosciences. A wide range of nanofabrication problems were taken into consideration for various geometric configurations and an extraordinarily extensive range of applications materials. Consequently, a wide range of materials were used to conduct

nanoelectronics, nanophotonics, nanomechanics, nanocatalysis, nanoantennae, and nanosensors.The materials employed for applications and the geometries required for next-generation uses in nanofabrication were practically as varied as the spectrum of roots towards these structures [1–14]. One can categorize the approaches as either "bottom-up" or "top-down."The term "top-down fabrication" describes techniques where a macroscopically dimensioned material, like a thin film with implanted flaws, is the starting point. Afterward, the term "top-down" described methods using focused ion beam lithography (FIB) or electron beam lithography (EBL). In some instances, bigger structures are carved into nanostructures using concentrated electrons or ions. On the other hand, the bottom-up method starts with smaller units and builds nanostructures from them. It has been established that as nanotechnology advances, both the quantity and significance of nanofabrication techniques will increase significantly in the upcoming years.

The motivation of this investigation was carried out by calculation of bulk electronic properties of 2D nanostructure with an integrated defect. The matching method [15-22]is used in the hopping integral model for nearest neighbors to calculate the dispersion branches in the considered system model of low dimension system. The calculation of the coefficient of transmission was completeness with reflection, associate electronic conductance, and density of states of bulk irreduciblesites. Thermal electronic conductivity was determined as an important physical measurable quantity related to the reliability of electronic devices. The reduction of the size of the system and the presence of various defects [23-35] affected the thermal electronic properties and disordered structures of low dimensionality. In this work weuse the matching approach and Landauer-Büttiker formalism, to describe the impacts of symmetric breaking on scattering and confinement of energy on the behavior of 2D nanostruc*ture*[36,37].Also, the different coefficients and electronic total transmittance, and thermal electronic conductivity of the perturbed system weredetermined and analyzed.Furthermore,to determine the state density we use the function of Green. In section2, the theoretical model and electronic dynamic were examined in bulk. In section 3,the analytical approach of electronic wave scattering was presented for inhomogeneity. In section 4, the thermal conductivity associated with the total transmittance of the system was studied.In section 5, the Green functions formalism was described and used for the calculation of state density associated witha localized state of irreducible sites. In section 6, numerical results were presentedwith discussions of different numerical results as a function ofthe hopping integral inthe neighborhood ofthe perturbed area. In section 7, general conclusions were presented.



**2.Formalism and system model**

The analytic formalism was applied tothe perturbed quantic 2D nanostructure represented in Fig.1.

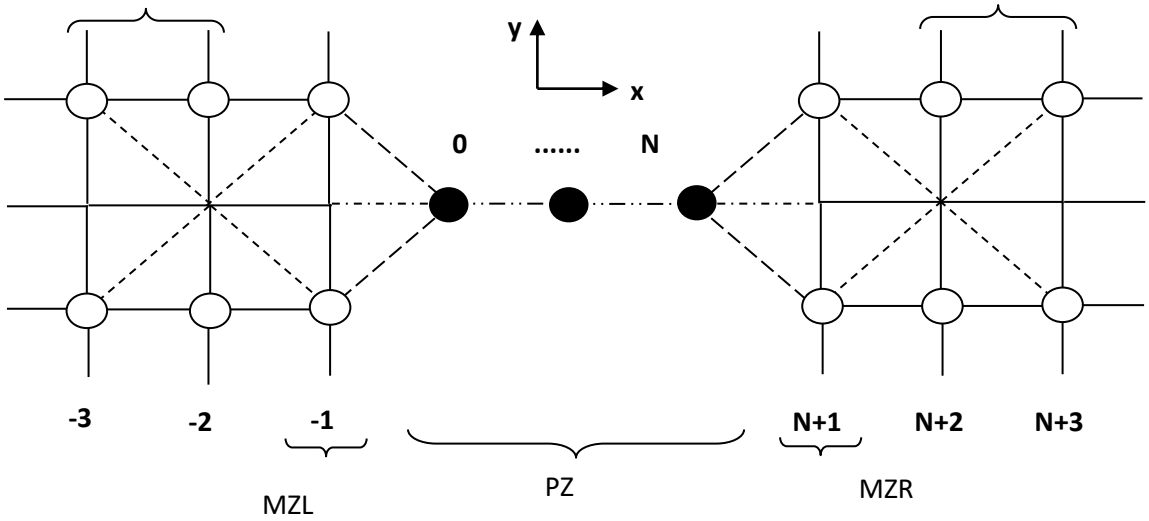


**Fig.1**: The Studied System model

The tight-binding (TB) or atomic orbital (AO) methods area more adequate approach used in this work. Since the pioneering work of Slater and Koster [39], the TB method has been extensively applied to semiconductors. Several different tight-binding Hamiltonians have been proposed in the past to solve various problems by using the economically realistic approach. Also, the matrix elements of Hamiltonian coupled with nearest neighbor orbitals wereexplained. To trace back the initial formulation in Tigh Binding Approximation (TBA) theory[40-43], the secular single-particle equation was performed byusing the tight-binding approximation and the electron transport in 2D nanostructure can be described in quantum mechanics by the Schrödinger equation as a single secular particle:

$$H\left|\psi_k(\vec{r})\right\rangle = E\left|\psi_k(\vec{r})\right\rangle \quad (1)$$

$\Psi_k$ : is the system's wave function of state *k.*



*E:* the energy of state *k.*

*H:* Hamiltonian

Where the base of atomic orbitals that overlapped or "hybridized" was used as;

$$|\Psi_n\rangle = \sum_{i,n} C_{in}\, e^{\vec{k}.\vec{r}} / \phi_n^i \quad (2)$$

$C_{in}$ denoted the orbital coefficients where *n*was the number of atoms in the unit cell and *i* was the number of orbitals (*i*=s). The atomic orbital functions are considered orthogonal;

$$\left\langle \phi_n^i \middle| \phi_{n'}^i \right\rangle = \delta_{n,n'} \quad (3)$$

Where

$$\delta_{n,n'} = \begin{cases} 1 & if \quad n = n' \\ 0 & if \quad n \neq n' \end{cases} \quad (4)$$

And the Hamiltonian system was written:

$H=H_0+V$(5)

$H_0$: the kinetic energy of nearest hybrid neighbors.

*V:* the potential energy matrix.

The Schrödinger equation became:

$$\left\langle \phi_n^i \middle| (H_0 + V) \middle| \psi \right\rangle = E \left\langle \phi_n^i \middle| I \middle| \psi \right\rangle \quad (6)$$

In the (TB) approximation, the nearest neighborswere considered as follows:

$C_{n,s}$ ,$C_{n+1,s}$, $C_{n-1,s}$ ,$C_{n,s+1}$ ,$C_{n-1,s+1}$ ,$C_{n+1,s+1}$; and the others were avoided. Equation (7) became;

$$H_{ij} c_{n-1,s} + (\varepsilon_i + V - E) c_{n,s} + H_{ij} c_{n+1,s} + H'_{ij}\, c_{n,s+1} = 0$$

$$H_{ij} c_{n,s} + (\varepsilon_i + V - E) c_{n,s+1} + H_{ij} c_{n-1,s+1} + H_{ij} c_{n+1,s+1} = 0 \quad (7)$$

With $\varepsilon_i$ : The energy of orbit *i.*

$H_{ij}$: the matrix of overlap elements between atom n and n'.

For the electronic structure ofthe system's bulk presented in Fig.1, with the introduction of Bloch's theory; $c_{n\pm1} = e^{\pm i\varphi_\alpha} c_n$ , where $e^{\pm i\varphi_\alpha}$ was the phase translation factor along a direction"α", which required a complete calculation of the bulk dispersion. Otherwise, Eq (7) presented the differentEigenvalues andthe propagation mode was extractedunder the condition given by

*| Z | = 1*. Also, the eigenstatesatisfied the condition *| Z | < 1*was determinedto compute the evanescent eigenstate. On the other hand, the system provided by Eq (6) of defect area generated a rectangular Hamiltonian matrix. In this situation, the Hamiltonian matrix contained an unbalanced number of unknown variables concerningthe number of secular equations. Therefore, a direct solution was not possible. An adequate method such as the phase field matching theory (PFMT) was used for this approach. It is an analytical approach that can determine the physical quantities characterized by disordered systems. It has

been introduced as a powerful method used to study the equilibrium of static structure of 2D semi-infinite crystal lattice and low-dimensional systems withintegrated defects.

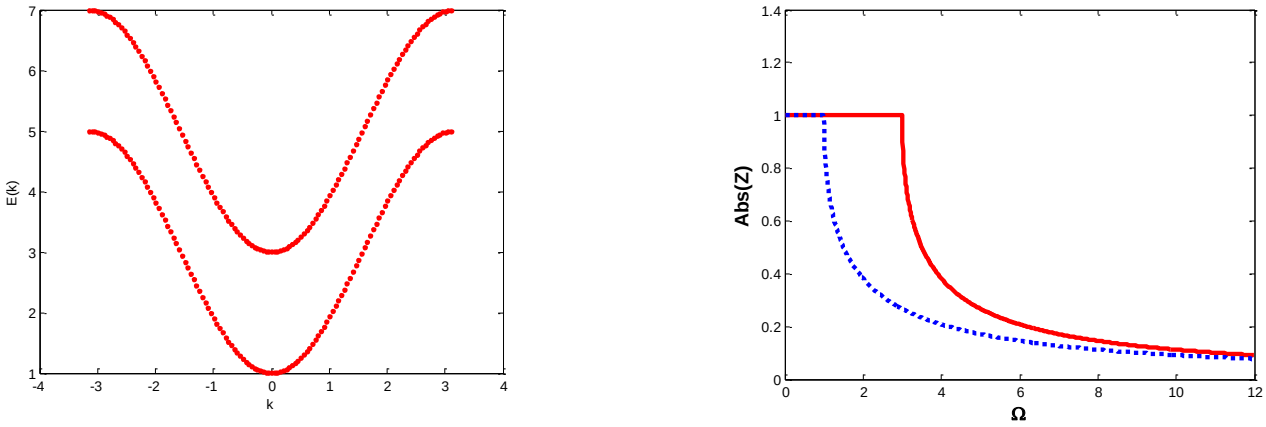


**Figure.2:**Representation of the dispersion curve



$\Omega(\Phi_x)$ for2D system in the bulkFigure.3: The variation of absolute valuephase factor Z
With$\varepsilon_s = energyofsiten$ blue eigenstate1 and (green color) eigenstate2
V= interacted potential
E=Energy of the system
$H_{ss}$=hopping integral

$$\Omega = \frac{\epsilon_{S+V-E}}{H_{SS}}$$

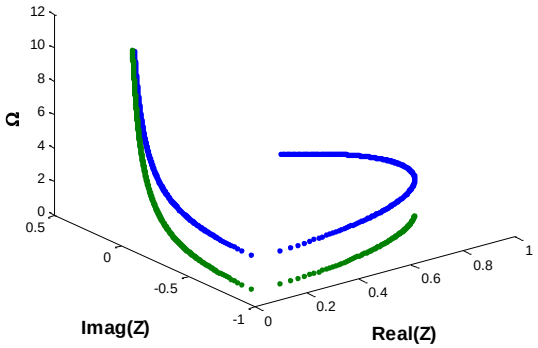


**Figure.4** The variation of 3D phase factor as a function of dimensionless frequencies and the parameters of studied system in the bulk

**3.Electronic ScatteringAt The Defect**

To determine the electronic matrix of defect, the Tight Binding method was used for inhomogeneous 2D nanostructure in the nearest neighborhoodapproximationas follows:

$C_{n,s}$ ,$C_{n+1,s}$, $C_{n-1,s}$ ,$C_{n+2,s}$ ,$C_{n-2,s}$ ,$C_{n,s+1}$ ,$C_{n+1,s+1}$ ,$C_{n-1,s+1}$ ,$C_{n+2,s+1}$ ,$C_{n-2,s+1} \neq 0$
; and the others are void. Equation (8) became;

$$H_{ij}c_{n-1,s}+(\varepsilon_i+V-E)c_{n,s}+H_{ij}c_{n+1,s}+H'_{ij}c_{n,s+1}=0$$
$$H_{ij}c_{n,s}+(\varepsilon_i+V-E)c_{n+1,s}+H_{ij}c_{n+2,s}+H_{ij}c_{n+1,s+1}=0$$
$$H_{ij}c_{n-2,s}+(\varepsilon_i+V-E)c_{n-1,s}+H_{ij}c_{n,s}+H_{ij}c_{n-1,s+1}=0$$
$$H_{ij}c_{n-1,s+1}+(\varepsilon_i+V-E)c_{n,s+1}+H_{ij}c_{n+1,s+1}+H'_{ij}c_{n,s}=0$$
$$H_{ij}c_{n,s+1}+(\varepsilon_i+V-E)c_{n+1,s+1}+H_{ij}c_{n+2,s+1}+H_{ij}c_{n+1,s}=0$$
$$H_{ij}c_{n-2,s+1}+(\varepsilon_i+V-E)c_{n-1,s+1}+H_{ij}c_{n,s+1}+H_{ij}c_{n-1,s}=0 \quad (8)$$

The rectangular matrix obtained of dimension (6x10) cannot determine the eigenvalues and eigenvectors. Therefore, the adapted matching method was used to resolve the problem. Also, the reflected $\vec{u}_r$ and transmitted waves $\vec{u}_t$ were developed as a linear combination of vectors to define two finite spaces based oneigenstates. The dimensions of unit vectors were related to the number of propagating modes obtained during the study of two perfect waveguides based on the following:

$$C(n,m)=\left[Z(\nu')\right]^n . p(\alpha,\nu')+\sum_{\nu} R_{\nu\bar{\nu}} .\left[Z(\nu)\right]^{-n} . \vec{p}(\alpha,\nu) \qquad \text{Where } n<-2 \quad (9$$

The displacements of the sites to the right of the defect are written as follows:

$$C(n,m)=\sum_{\nu} T_{\nu\bar{\nu}} .\left[Z(\nu)\right]^n . \vec{p}(\alpha,\nu) \qquad \text{Where } n>2 \quad (10)$$



Also, the quantities $T_{\nu\bar{\nu}}$ and $R_{\nu\bar{\nu}}$ are complex factorsof standardization of the ratio of a group of velocities that allowed the obtaining of certain physical quantities of interest. The Harrison coefficient for the site located outside the region of the defect (LR) can be expressed by the matching method[17,18]. This can beexpressed by the superposition of the incident wave and reflected part of the electronic wave at the same frequency see equation (9). For the site of the right matching region, the Harrison coefficient is presented in equation (10) only forthe transmitted part of the electronic wave.

As depicted in Figure (1a-1c), the Landauer approach which relates the conductance ofthe system with the probability of transmission of conduction channels are the transmission coefficients ofan incident wave i into the eigenstate$\nu$ =1.

The quantities allowedthe calculationof coefficients of reflections and transmissions. This can be followedby the normalized ratio of the group of velocities to ensure the conservation of energy and unitarity of the sum of reflected and transmitted parts. Therefore, three cases of waves were produced from the left side of the defect according to the eigenstate.The coefficient of reflection is given by the following relation:

$$r_{\nu\bar{\nu}}=\left(\frac{W_{g\nu}}{W_{g\bar{\nu}}}\right).\left|R_{\nu\bar{\nu}}\right|^2 . \quad (11.a)$$

And the coefficient of transmission can be expressed by the relation:

$$t_{\nu\bar{\nu}}=\left(\frac{W_{g\nu}}{W_{g\bar{\nu}}}\right).\left|T_{\nu\bar{\nu}}\right|^2 \qquad (11.b)$$

Where $W_{g\nu}$ denoted the group speed corresponded to the eigenstate$\nu$

To describe the global transmission of electronic waves through the system, electronic conductance was defined by analogy with relation to the scattering phenomena. The electronic conductance was expressed as a function of incident energy and the angle of incidencewas noted as $\sigma$ ($\Omega$). It wasgiven by the sum of transmission coefficients of propagating modes of the perfect system. The total electronic-wave conductance of system $\sigma$ ($\Omega$) was calculated as a useful quantity corresponding to an experimentally measurable observable such as heat transfer.

Diffusion-related functions such as reflection and transmission depend ofdimensionless frequencies are shown in Figures.4a and 4c for a propagating direction correspondingwith the angle of incidence $\phi_y = \phi_z = 0$.

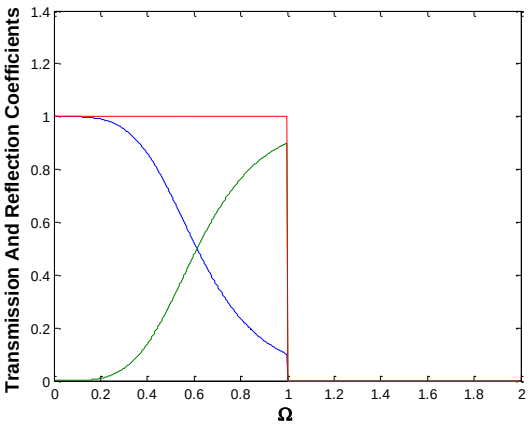


Figure.5:Curves of transmission and reflection coefficients of mode one as a function of dimensionless frequencies as a function of dimensionless frequencies
and parameters of the perturbed zone

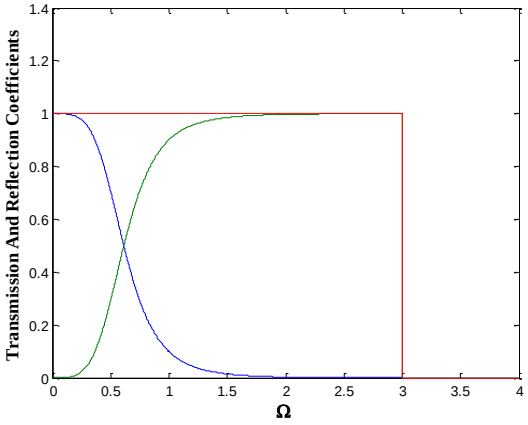


Figure.6:Curves of transmission and reflection coefficients of mode two
and parameters of the perturbed zone



**4.Electronic Heat Transport**

Since conductance was the most naturally occurring measurable quantity for the movement of electrons, electronic conductance (K) was used in the current work to characterize electronic transport. The natural motion of electrical current carriers in matter is generally involved in a proper description of electronic transport that determines the electronic conductance in solids. Nevertheless, when a material's dimension decreases, electrons' typical behavior could alter. The characteristics of lengths that are thought of as the mean free path of electrons (L) determined the type of electron transport. This can be compared to the material's diameter and length, and it was defined as the distance between two consecutive electron collisions with defects or phonons.The crucial factor in determining thermal conductivity was the electrical conductance computation. This method relied heavily on the waveguide conductance σ(ω), Fermi-Dirac distribution, and velocity of each mode. For the net heat current,Q12, maintained between slightly differing temperatures T+ΔT > T across the defect between the two ends of the waveguide. As a result, the thermal conductivities are shown in relation to group velocity and temperature. The heat transport contributions grew until they reached a maximum value, as indicated by the calculation curves. As a result, there is a greater electron excitation from the valence band to the conduction band, and every eigenstate has a unique electron number. Thus, the performance of electronic dispostif was decreased by the heat effect. This work's thermal. The waveguide conductance $\sigma(\omega)$, Fermi-Dirac distribution $n(T,\omega_j(q))$, and velocity of each mode $\upsilon_{gj}$ played an essential role in the whole analysis. For the net heat current, $\delta Q_{12}$, across the defectbetween the two ends of the waveguide, held between slightly different temperatures *T+ΔT > T* as follows:

$$\partial Q_{12} = \frac{1}{\ell}\sum_j \frac{1}{(2\pi)^2}\int dq \upsilon_{gj}(q)\hbar\omega_j(q)\sigma_j(\omega_j,q) \times \frac{\partial n(T,\omega_j(q))}{\partial T} \quad (12)$$

For ferromagnetic metals, the electronic and phononic contributions generally guarantee thermal conductivity, not the magnetic ones. The majority of charge carriers supplied by the two-electron modes carried the heat in this work, which examined the electronic contribution. Figure (11)

shows the thermal conductivities as a function of group velocity and temperature. The heat transport contributions grew until they reached a maximum value, as indicated by the calculation curves. Thus, in the presence of an electron number and unique feature, this can be explained by the excitation of electrons from the valence band towards the conduction band. Therefore, thermal runaway caused the thermal effect to lower electronic system performance..

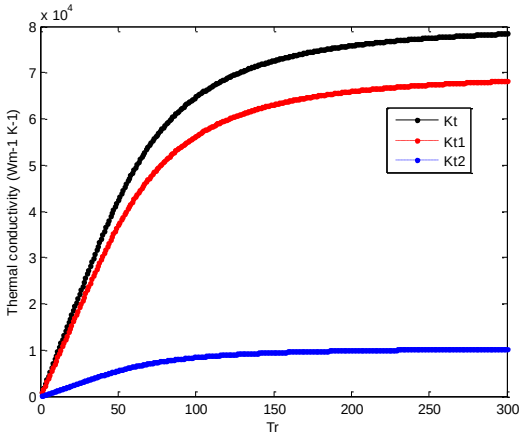


178

**Figure.7:**Curves of thermal conductivity as a function of temperature and parameters of the studied system

**5. State densities of the localized state**

The most adapted and appropriate method of calculation of spectral and state density (EDOS) of irreducible sites of the system model wasthe Green Function associated with the matching formalism,expressed as follows [44]:

$G(\Omega + i\varepsilon) = [\, D(\eta, \phi_x, \phi_y, \gamma, \Omega, ) \,]^{-1}$(13)

The EDOS per atomic site *p*was obtained by the following equation.

$$D_p(\Omega) = -\frac{1}{\pi}\sum_{\alpha}\sum_{\phi x \phi y} \lim_{\varepsilon \to 0^+} \left\{ \mathrm{Im}\left[ G_{\beta\beta'}^{pp'}(\phi_x, \phi_y, \gamma, \Omega + i\varepsilon) \right] \right\} \quad (14)$$

The behavior of 2D nanostructure boundaries' irreducible site's DOS was ascertained in relation to the perturbed domain parameters and incident energies . Figures (8a-8d) display the state density curves linked to localized states as a function of the defect system's parameters and reduced frequency. Additionally, these curves covered the bulk mode propagation range, which is represented by the frequency interval $\Omega \in [0, 4]$. There were multiple resonance peaks that varied in width and height. In the first Brillouin zone of the system model, the evolution of the state density curves for various irreducible sites was expressed as a function of frequency Ω in international units. The spectra showed the peaks and oscillations with frequencies range corresponding to the interval of dispersion branches of perfect structure. The oscillations were due to the coupling between states located in the system model. Hence, this quantity was commonly used in experimental physics since has directly measurable electronic systems by thermal runaway.

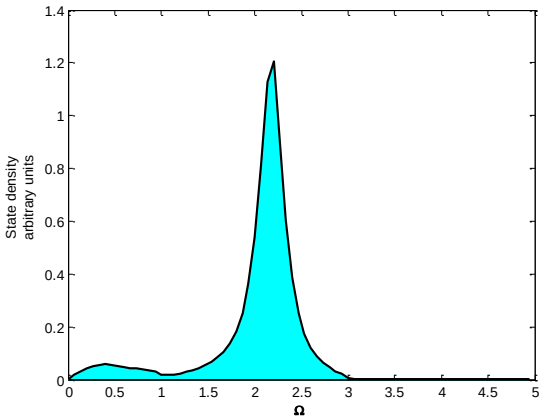


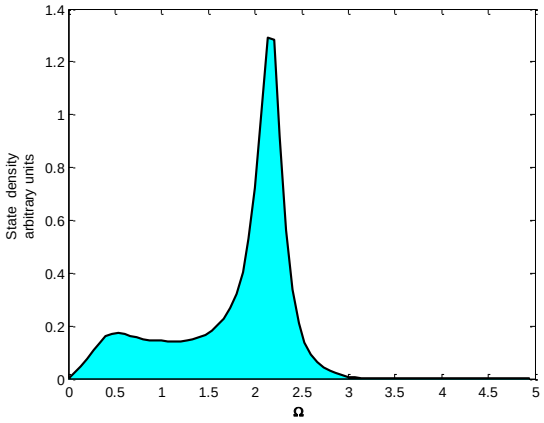


Figure.8a: The calculated EDOS of atomic site 1Figure.8b: The calculated EDOS of atomic site2

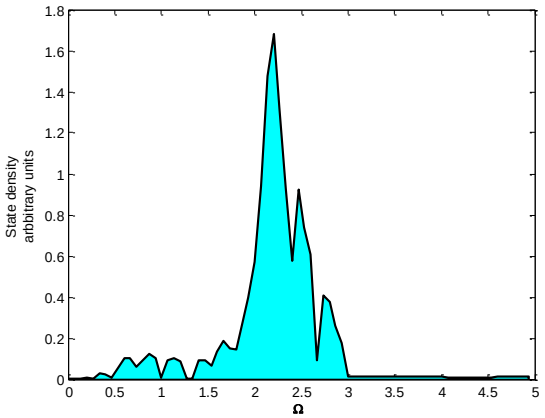


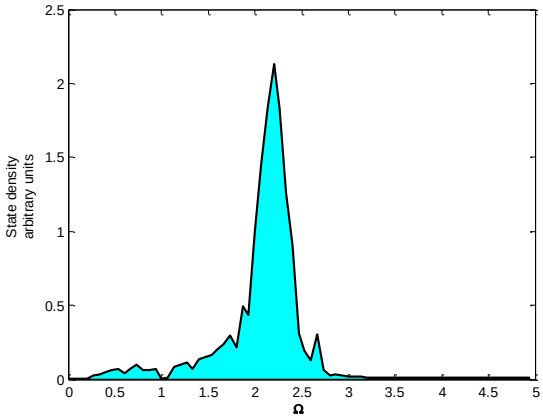


Figure.8c :The calculated EDOS of atomic site 3 Figure.8d: The calculated EDOS of atomic site 4



**6.Results and discussion**

The results are presented for the choice ofϕx= 0, In this case, the propagating electron eigenstate appearedin the intervalsof Ω1 = [0, Ω1,max = 5] and Ω2 = [3, Ω2,max = 7]. The typical electronic dispersion branches of j = 1 and j= 2 are presented in Figure 2. There was one acoustic modeofj= 2and frequency tended to zero when ϕx tended to zero. On the other hand, for j=1,the mode was optical different from zero for ϕx=0. The two-phase factors are presented in Fig.3 and stand in domain frequencies ofΩ1 = [0, Ω1,max = 2.90] and Ω2 = [0 Ω2,max = 0.90],respectively.The other frequencies have vanished. The presentation in 3D and Fig.4were more complete andproduced the phase and modulus of mode.The transmission and reflection coefficients corresponding to the two electronic eigenstates of the system model are presented in Figures 5 and 6. So, the transmission and reflection across sections verified the unitary condition ofthe scattering matrix for common usein numerical calculation. The transmission curve per electroneigenstate for the electronic 2D nanostructurewas presented for comparison of cases. It is important to distinguish between the two eigenstates.The coefficients of transmission and reflection of optical eigenstates stand were in the interval frequencies and corresponded to propagating mode of Ω1 = [0, Ω1,max = 2.90] and vanished for all other frequencies. The other coefficient corresponding to the acoustical statewas stand in the interval frequenciesof Ω1 = [0, Ω1,max = 0.90] and vanished everywhere else. Also, the coefficient of transmission was

decreaseduntil the vanishment at the limit band frequencies ofeigenstates.This was due to its interaction with the system and loss of energy through it. On the other hand,the reflection coefficient was increased up to the limit of the propagation interval of eigenstates.The thermal conductivities *Kj*of electronic eigenstateswere calculated in particular from equations (11) as a function of temperature, Fermi distribution, and total transmittance or the coefficient of transmission of eigenstates. The calculated *Kj*(*T* ) of odd-numbered electronic state *{j* = 1*,* 2*}* is presented in Figure 7.The greater thermal conductivity was related to the nature of the material.On the other hand, the smaller was related to the more insulating material.Therefore, the thermal conductivity of materials characterized indicated the amount of heat propagated by thermal conduction.Electrons and phonons are the particles responsible for thermal conductivity. The eigenstate 1 was more energetic than the two(2) and their contribution to thermal conductivity was additive. In physics, thermal conductivity was the quantity introduced to quantify theability of the body to conduct heat. It represented the quantity of heattransferred per unit area and per unit of time under the action of the temperature difference between the two ends of a sample of the body in the presence of a temperature gradient. Depending essentially on the nature of materials considered, it was generally found in directrelation with the electrical conductivity of the body. This propertywas relatedto the free electrons in the body which are most often associated with heat transfers. The figures 8a and 8f present the electronic density (EDOS). The number of distinct states at a given energy level as electrons are occupied by the number of electron states per unit volume and per unit energy is the basic definition of the electronic density of states (EDOS). Furthermore, these functions also influenced bulk characteristics of conductive solids, such as specific heat, paramagnetic susceptibility, and other transport phenomena. The general distribution of states as a function of energy was determined through EDOS calculations, which can also be used to calculate the distance between energy bands in semiconductors. Given the parameters of the perturbed domains and incident, the EDOS of the irreducible site of the behavior of 2D nanostructure with integrated defect system boundaries was calculated. The curves of state density associated with the localized states are presented in Figures 8.a-8.d as a function of dimensionless frequencies and parameters of the system. These curves extended over a frequencyof interval of$\Omega$ =[0, 4] corresponded to the propagation range of bulk eigenstates. It presented several peaks of resonances with different heights and widths. The curve related to site1 presented the feathers at a different dimension of dimensionless frequencies as depicted in table1.The feathers of site 2 were presented in table2So,and the different peaks and their characteristics of sites 3 and 4 are presented in Tables 3 and 4, respectively.Hence, the electronic state densities of sites 5 and 6 were similar to those of sites 3 and 4, respectively.The evolution of the curves of state densities of different irreducible sites is expressed in arbitrary units as a function of normalized frequency $\Omega$ in the first Brillouin zoneof the 2D nanostructure. The spectra showed the peaks and oscillations spanned by a frequency range that corresponded to the interval of dispersion branches of perfect structure[0,3]. These oscillations were due to the coupling between the states located in the behavior of inserted atomic implanted defect. This quantity was commonly used in experimental physics since it was directly measurable.

**7. General Conclusions**

The numerical results of the analytical study of the electronic dynamic and scattering of atomic 2D nanostructure with integrated atomic defects were presented. The dispersion branches of bulk, resonances, and EDOS were calculated by the system model. The characteristics of different properties and coefficients of transmission, reflection, and electronic transmittance of EDOS were related to the structural order of system models and their characteristicsand electronic properties. The results were similar to other analytical models and empiric values. This formalism was used to determinethe other thermophysical properties of the system. Thus, the thermal conductivity associated with the transmittance of the system was determined as a function of temperature and parameters of the behavior of the perturbedzone

**Acknowledgments**
We would like to thank Ahmed Draia University for the working conditions made available to us

**References**

[1]. A. Abdurahman, A. Shukla and M. Dolg. Ab initio many-body calculations of static dipole polarizabilities of linear carbon chains and chainlikeboron clusters. Phys Rev B, vol. 65, page 115106, 2002,https://doi.org/10.1103/PhysRevB.66.155423
[2] .N. Agra¨ıt, A. Levy-Yeyati and J. M. van Ruitenbeek. Quantum properties of atomic-sized conductors. Phys Rep, vol. 377, pages 81–279, 2003, https://doi.org/10.1016/S0370-1573%2802%2900633-6
[3].E. Akt¨urk, C. Ataca, and S. Ciraci. Effects of silicon and germanium adsorbed on graphene.ApplPhysLett, vol. 96, page 123112, 2010,https://doi.org/10.1063/1.3368704
[4] .T. Ando. Quantum point contacts in magnetic fields. PhysRev B, vol. 44, pages 8017–8027, 1991,DOI:https://doi.org/10.1103/PhysRevB.44.8017
[5] C. Ataca, E. Akt¨urk, H. S¸ahin and S. Ciraci.Adsorption of carbon adatoms to graphene and its nanoribbons. J ApplPhys, vol. 109, page 013704, 2011,https://doi.org/10.1063/1.3527067
[6]. P. Avouris, Z. Chen and V. Perebeinos.Carbon-based electronics.NatNanotechnol, vol. 2, pages 60–615, 2007.doi: 10.1038/nnano.2007.300. Epub 2007 Sep 30.
[7] .A. A. Balandin, S. Ghosh, W. Z. Bao, I. Calizo, D. Teweldebrhan, F. Miao and C. N. Lau. Superior Thermal Conductivity of Single-Layer Graphene.Nano Lett, vol. 8, pages 902–907, 2008. DOI: 10.1021/nl0731872
[8]. E. Bekaroglu, M. Topsakal, S. Cahangirov and S. Ciraci. First-principles study of defects and adatoms in silicon carbide honeycomb structures. PhysRev B, vol. 81, page 075433, 2010,DOI:https://doi.org/10.1103/PhysRevB.81.075433
[9]. J. Bettini, F. Sato, P.Z. Coura, S.O. Dantas, D.S. Galvao and D. Ugarte. Experimental realization of suspended atomic chains composed of different atomic species. Nature Nanotechnol, vol. 1, pages 182–185, 2006,doi: 10.1038/nnano.2006.132. Epub 2006 Nov 19.
[10] .F. Bloch. Uber die Quantenmechanik der elektronen in kristallgittern ¨ . Z Phys, vol. 52, pages 555–600, 1929.http://dx.doi.org/10.1007/BF01339455
[11]. T. B. Boykin and G. Klimeck. The discretized Schrödinger equation and simple models for semiconductor quantum wells. Eur J Phys, vol. 25, pages 503–514, 2004,DOI: 10.1088/0143-0807/25/4/006
[12] T. B. Boykin and G. Klimeck. The discretized Schrödinger equation for the finite square well and its relationship to solid-state physics. Eur J Phys, vol. 26, pages 865–881, 2005.**DOI** 10.1088/0143-0807/26/5/020
[13]. T. B. Boykin, M. Luisier, G. Klimeck, X. Jiang, N. Kharche, Y. Zhou and S. K. Nayak. Accurate six-band nearest-neighbor tight-binding model for the π-bands of bulk graphene and graphenenanoribbons. J ApplPhys, vol. 109, page 104304, 2011,https://doi.org/10.1063/1.3582136
[14]. O. Brovko, P.A. Ignatiev and V.S. Stepanyuk. Confined bulk states as a long-range sense for impurities and a transfer channel for quantum information.PhysRev B, vol. 83, page 125415, 2011,DOI:https://doi.org/10.1103/PhysRevB.83.125415
[15].B. Bourahla, A. Khater and M. AbouGhantous, EPJ Web of Conferences , published by EDP Sciences, 2012,DOI: 10.1051 epjconf 201 / 22 29 00011 (2012) 900011
[16] Elie A. Moujaes A. Khater , M. AbouGhantous, V. Ashokan, MagnonicballistictransportacrossFe-Nialloynanojunctionsbetween Fe/ColeadsusingPhaseFieldMatchingandIsingEffectiveFieldTheory approaches,Materialia,Volume 4, December 2018, Pages 373-387 DOI:10.1016/j.mtla.2018.10.012

[17].Doried Ghader, Vinod Ashokan, Michel Abou Ghantous andAntoine Khater ,Spin waves transport across a ferrimagnetically ordered nanojunction of cobalt-gadolinium alloy between cobalt leads, The European Physical Journal B volume 86 ,180 (2013), https://doi.org/10.1140/epjb/e2013-30994-5
[18].J. Szeftel, A. Khater, Calculation of surface phonons and resonances: the matching procedure revisited: I,J. Phys. C Solid State Phys. 20, 4725 (1987), **DOI** 10.1088/0022-3719/20/29/010.
[19].T.E. Feuchtwang, Phys. Rev. 155, 731 (1967).
[20]B. Bourahla, A. Khater, R. Tigrine, O. Rafil, M. Abou Ghantous, J. Phys.: Condens. Matter 19, 266208 (2007)
[21].B. Bourahla, A. Khater, R. Tigrine, Thin Solid Films 517, 6857 (2009).
[22].A. Khater, M. Belhadi, Surface Rev. Lett. 16, 271 (2009).
[23]. P. L. Euen. Nanotechnology: Carbon-based electronics. Nature, vol. 393, pages 15–16, 1998.
[24] .X. Fan, Z. Shen, A. Q. Liu and J. L. Kuo. Band gap opening of grapheme by doping small boron nitride domains.Nanoscale, vol. 4, pages 2157–2165, 2012.
[25]. A. Fellay, F. Gagel, K. Maschke, A. Virlouvet and A. Khater. Scattering of vibrational waves in perturbed quasi-one-dimensional multichannel waveguides. Phys Rev B, vol. 55, pages 1707–1717, 1997.
[30]. S. F¨olsch, P. Hyldgaard, R. Koch and K.H. Ploog. Quantum confinement in monatomic Cu chains on Cu(111). Phys Rev Lett, vol. 92, page 056803,2004.
[31]. P. Fuentealba. Static dipole polarizabilities of small neutral carbon clusters Cn (n 6 8).Phys Rev A, vol. 58, pages 4232–4234, 1998.
[32]. A. K. Geim and K. S. Novoselov. The rise ofgraphene. Nature Mater, vol. 6, pages 183–191, 2007.
[33] A. Khater, M. Belhadi , and M. AbouGhantous ,Phonons heat transport at an atomic well boundary in ultrathin solid film Eur. Phys. J. B 80, 363–369 (2011) [Guisinger& Arnold 2010] N. P. Guisinger and M. S. Arnold. Beyond Silicon: CarbonBased Nanotechnology. MRS Bull, vol. 4, pages 273–279, 2010.
[34].M. Y. Han. Energy band-gap engineering ofgraphenenanoribbons. Phys Rev Lett, vol. 98, page 206805, 2007.
[41]. M. Y. Han. Electron transport in disorderedgraphenenanoribbons. Phys Rev Lett, vol. 104, page 056801, 2010.
[35]. I. D. Hands, J. L. Dunn and C. A. Bates. Visualization of static
Jahn-Teller effects in the fullerene anion C- 60. PhysRev B, vol. 82, page 155
[36]. R. Landauer, IBM J. Res. Dev. 1, 223 (1957)
[37]. R. Landauer, Philos. Mag. 21, 863 (1970)
[ 38]. Büttiker, Phys. Rev. Lett. 57, 1761 (1986)
[39] J.C.Slater and G.F. Koster, Simplified LCAO method for the periodic potential problem, Phys. Rev,vol 94,N°6.(1954)1498-1524.
[40]. W.A. Harrison. Why tight-binding theory? Solid State Commun, vol. 124,
pages 443–447, 2002

[41] W. A. Harrison. Elementary electronic structure. World Scientific, Singapore, 2004.
[Havu et al. 2006] P. Havu, V. Havu, M.J. Puska, M.H. Hakala, A.S. Foster and R. Nieminen. Finite-element implementation for electron transport in nanostructures. J ChemPhys, vol. 124, page 054707, 2006

[42].D.Szczésniak and A. Khater. Electronic conductance via atomic wires: a phase field matching theory approach. EurPhys J B, vol. 85, page 174, 2012.
[43]. D.Szczésniak, A. Khater, Z. B¸ak, R. Szcz¸e´sniak and M. AbouGhantous. Quantum conductance of silicon-doped carbon wire nanojunctions.
[44]. A. Khater and H. Grimech, surface sci . 251, 381 (1991).
[45].R.Tigrine, A. Khater, B. Bourahla, M. AbouGhantous and O. Rafli. Magnon scattering by a symmetric atomic well in free standing very thin magneticfilms.EurPhys J B, vol. 62, pages 59–64, 2008.